Am J Transl Res 2020;12(6):2860-2874
www.ajtr.org /ISSN:1943-8141/AJTR0110780

Original Article

LncRNA PVT1 epigenetically stabilizes and post-transcriptionally regulates FOXM1 by acting as a microRNA sponge and thus promotes malignant behaviors of ovarian cancer cells

Ke Yi[1,2], Minmin Hou[1,2], Jialing Yuan[1,2], Lingyun Yang[1,2], Xi Zeng[1,2], Mingrong Xi[1,2], Jie Chen[1,2]

[1]Department of Obstetrics and Gynecology, West China Second University Hospital, Sichuan University, No. 20, Section 3, RenminNanlu Road, Chengdu 610041, Sichuan, China; [2]The Key Laboratory of Birth Defects and Related Diseases of Women and Children (Sichuan University), Ministry of Education, Chengdu 610041, Sichuan, China

Received November 15, 2019; Accepted March 21, 2020; Epub June 15, 2020; Published June 30, 2020

Abstract: Accumulating evidence demonstrates that long noncoding RNAs (lncRNAs) may be involved in the regula tion of cancer biology. PVT1, which is overexpressed in tumor samples, acts as an oncogenic promoter in several kinds of cancers, including ovarian cancer. However, the mechanisms of its regulation of malignant behaviors in ovarian cancer remain largely unknown. In this study, the expression of PVT1 in several ovarian cancer cell lines was analyzed by qRT-PCR. The effect of PVT1 on malignant behaviors, including cell proliferation, migration and invasion, was analyzed. The posttranscriptional regulation of FOXM1 by PVT1 was analyzed by western blotting. The results illustrated that PVT1 acted as a sponge and bound miR-370 on two binding sites. The expression of PVT1 positively regulated malignant behaviors in ovarian cancer cells, including cell proliferation, migration and invasion, which could be reversed by the introduction of miR-370 mimics. Sponged miR-370 failed to posttranscriptionally regulate FOXM1, which resulted in the promotion of malignant behavior. PVT1 was also found to bind to FOXM1 directly and stabilize the FOXM1 protein. The promoting effect of PVT1 on malignant behaviors and chemoresistance to cisplatin could be reversed by knockdown of FOXM1 and introduction of miR-370 mimics. Together, these results suggest that lncRNA PVT1 promotes malignant behavior and induces chemoresistance in ovarian cancer by epigenetic and posttranscriptional regulation of FOXM1.

Keywords: Long non-coding RNAs (lncRNAs), ovarian cancer, FOXM1, microRNA sponge, malignancy

Introduction

Long noncoding RNAs (lncRNAs) are a class of RNAs consisting of 200-100,000 nt that play many roles in physiological processes. LncRNAs are also widely involved in human diseases, including cancer [1]. Numerous well-identified lncRNAs have been revealed to play critical regulatory roles in tumorigenesis, progression and metastasis, including metastasis-associated lung adenocarcinoma transcript 1 (MALAT-1) in breast cancer [2] and HOX transcript antisense RNA (HOTAIR) in pancreatic cancer [3]. More novel identified lncRNAs have also been reported to be tightly involved in regulatory processes of cancer cells, such as lncRNA 00239 in myeloid leukemia cells [4]. LncRNA PVT1, a recently identified lncRNA, has been shown to be abnormally upregulated in somatic malignancies and functions as a promotor of tumor growth in gastric cancer [5], colorectal cancer [6], and acute promyelocytic leukemia [7]. In all of these types of cancers, PVT1 has been reported as an oncogenic factor that promotes malignant behaviors. Although many interacting modulators of PVT1 have been found, including NOP2 [8], c-MYC [9] and FOXM1 [10], it is still unclear how PVT1 exerts its effects as a tumor promoter in these cancers. The identification of the mechanism by which PVT1 regulates its interacting partners would help elucidate its critical role in tumor progression.

Forkhead box M1 (FOXM1) is a member of the Forkhead box family, which can specifically bind to winged-helix DNA [11]. Under normal conditions, FOXM1 is critically involved in regulating embryogenesis [12] and organ development [13], and its upregulation has also been observed in various human cancers [14, 15]. In ovarian cancer, upregulated and activated FOXM1 has been reported to be positively associated with the majority of high-grade serous ovarian cancers, which is the most deadly ovarian cancer with poor prognosis [16]. In ovarian cancer, upregulation of FOXM1 results in promotion of cell proliferation, migration and invasion, but the exact molecular mechanism is unclear [17]. PVT1 directly binds to and stabilizes the FOXM1 protein. Moreover, PVT1 is then transcriptionally activated by FOXM1, by FOXM1 interacting with the PVT1 promoter region [10]. In this way, FOXM1 is epigenetically regulated by PVT1 via direct binding.

FOXM1 is also posttranscriptionally regulated by microRNAs, including miR-370 in ovarian cancer [18]. Chen and colleagues reported that by introducing miR-370, FOXM1 was knocked down, and consequently, cell proliferation, migration, invasion and epithelial-mesenchymal transition (EMT) were inhibited [18]. The circular RNA hsa_circ_0061140, which has been previously reported to be abnormally upregulated in ovarian cancer [19], acts as a sponge targeting miR-370 [20]. Hsa_circ_0061140 appeared to function as a competing endogenous RNA of miR-370 and thus regulated cell proliferation and other malignant behaviors, including migration, invasion and tumor formation in ovarian cancer via regulation of the miR-370/FOXM1 pathway mediating EMT. Interestingly, through bioinformatic prediction analysis, two predicated binding sites of miR-370 were observed on PVT1, which indicated that PVT1 potentially also acts as a regulator of FOXM1 by sponging miR-370. The identification of how PVT1 exactly regulates FOXM1 may help determine how the PVT1/FOXM1/miR-370 pathway mediates malignant behaviors in ovarian cancers.

In the present investigation, we bioinformatically predicted the binding sites of miR-370 on PVT1 and the biological significance of their interaction in ovarian cancer cell lines. Our results showed that PVT1 was upregulated in ovarian cancer cells and epigenetically and posttranscriptionally regulated the protein level of FOXM1. This study provides novel evidence that may further reveal the regulatory mechanism of PVT1 on FOXM1, which may aid in the development of effective therapeutic strategies for ovarian cancer therapy.

Material and methods

Cell culture

Human ovarian cancer cell lines, including SkOV3, OVCAR3, ALST and ES2, human ovarian cells, IOSE80, were purchased from the American Type Culture Collection (ATCC; Manassas, VA) and stored in our laboratory. All these cells were cultured in Dulbecco's modified Eagle's medium (SKOV3, OVCAR3 and IOSE80) or RPMI-1640 (ALST, ES2) supplemented with 5% fetal bovine serum (FBS; Thermo Scientific, Waltham, MA, USA). All cells were maintained in a 37°C humidified atmosphere of 95% air and 5% CO_2, and passaged every three days.

Prediction of miRNA targets

To predict binding microRNAs of PVT1, the bioinformatic tool (RegRNA2.0) was employed, and two binding sites for miR-370 and one binding site for miR-526-5p were detected.

Luciferase reporter assays

The human PVT1 RNA (1940 bp) were PCR-amplified from cDNA of SkOV3 cells, using primers containing flanking *Xho* I and *Sal* I recognition sequences (Fw: 5'-CCGCTCGAGCTCCGGGCAGAGCGCGTGTGGC-3'; Rev: 5'-CGCGTCGACTAGTAGAAAAAAGAATTTAATAGACAC-3'). The amplified products were ligated in the multiple cloning site of pmirGLO dual-luciferase miRNA target expression vector (Promega, Madison, WI, USA). The recombinant product (pmirGLO-PVT1, pmirGLO-PVT1-MUT1/3 or pmirGLO-PVT1-MUT2) was transfected into HEK293 together with 50 nM of miR-370-5p or miR-526-5p mimics purchased from RIBOBIO (Guangzhou, China) by using Lipofectamine 2000 (Life Technologies, Grand Island, NY, USA). 48-hour later, cells were lysed in passive lysis buffer (Promega, Madison, WI, USA), and luciferase activity was determined using the dual-luciferase assay kit (Promega, Madison,

WI, USA) in a GLOMAX 20/20 luminometer (Promega, Madison, WI, USA). To calculate the relative activity of luciferase reporter gene, the activity of luciferase normalized to *Renilla luciferase* was expressed as a percentage of relative luciferase units. All experiments were repeated three times.

Reverse-transcriptional quantitative polymerase chain reaction

To obtain total RNA, target cells were lysed by employing SoniConvert® tissue sonicator (UTL: http://www.doc-sense.com/index.html, DocSense, Chengdu, China) following manufacturer's instruction and isolated using TRIZol (Life technology, Grand Island, NY, USA). To evaluate microRNA expressing levels, the first-strand cDNA was synthesized from 1 ug of total RNA using the All-in-OneTM miRNA First-Strand cDNA synthesis Kit (RIBOBIO, Guangzhou, China). Quantitative PCR was performed with an All-in-One™ miRNA qRT-PCR Detection Kit (RIBOBIO, Guangzhou, China), and Applied Biosystems 7500 Real-time system (ABI 7500HT instrument) were used for measurement. The primers used in this research are also purchased from RIBOBIO, including miR-370-5p (Cat. No.: HmiRQP0456), miR-526-5p (Cat. No.: HmiRQP0612) and U6 small nuclear RNA (Cat. No.: HQP015877). To evaluate mRNA expressing levels, the first-strand cDNA was synthesized from 1 ug of total RNA using the First-Strand cDNA synthesis Kit (RIBOBIO, Guangzhou, China). Quantitative PCR was performed with a BlazeTaq™ SYBR® Green qPCR mix 2.0 kit (RIBOBIO, Guangzhou, China). The primers used in this research are also purchased from RIBOBIO, including PVT1 (forward 5'-TGGTGTTCCCCTTTTACTGC-3', reverse 5'-TGGTGAAACCCCGTCTCTAC-3'), FOXM1 (Cat. No.: HQP005712), β-actin (Cat. No.: HQP-108762).

CCK-8 analysis

Cells were suspended and adjust to 1×10^6 cells/ml. 10000 cells/well were seeded into a 96-well plate and allowed to attach overnight. 24-hour later, the Cell Counting Kit-8 (CCK-8, Sigma-Aldrich, St. Louis, MO, USA) prepared solution was added for a 2-hour co-incubation at 37°C avoid from light. A450 was detected by microplate reader (Synergy 2 Multi-Mode Microplate Reader; BioTek, Winooski, VT, USA) to determine the cell viability.

EdU staining

To image proliferating cells, the incorporation of 5-ethynyl-20-deoxyuridine (EdU) with an EdU Cell Proliferation Assay Kit (Ribobio, Guangzhou, China) was employed to stain proliferating cells. Briefly, 50 mM EdU was added into fresh medium for 4 h co-incubation with cells and then stained cells were fixed with 4% paraformaldehyde for 10 minutes at room temperature. Then, EdU staining was performed according to the manufacturer's protocol. Cell nuclei were stained with Hoechst33342 (Sigma) at a concentration of 1 mg/mL for 5 min at room temperature avoid from light. The proportion of cells incorporating EdU was determined using a X71 (U-RFL-T) fluorescence microscope (Olympus, Melville, NY).

Cell cycle analysis

To detect the proportion of cell cycle phases, the cells were suspended and washed with ice-cold PBS for three times. After pelleting, cells were fixed with ice-cold 70% ethanol at a concentration of 1×10^6 cells per ml. 12-hour later, cells were pelleted and washed with ice-cold PBS for three times, then cells were suspended with 5 μg/ml propidium iodide (PI, Sigma-Aldrich, St. Louis, MO, USA) for 10 min avoid from light. Then, without additional washes, stained cells were analyzed using 3 laser Navios flow cytometers (Beckman Coulter, Brea, CA, USA).

Migration and invasion

To evaluate the migration and invasion abilities, cells were suspended a plated into upper chamber (8-μm pore size; Corning Inc., Corning, NY. USA). For measuring migration ability, chamber was employed directly, for measuring invasion ability, chamber was coated with 0.8% of Matrigel (Sigma-Aldrich, St. Louis, MO, USA). 24-hour later, the cells on the lower face of chamber was fixed with 4% paraformaldehyde for 10 minutes at room temperature, and then stained with 0.25% crystal violet (Sigma-Aldrich). Five views of each chamber were imaged using a X71 (U-RFL-T) fluorescence microscope (Olympus, Melville, NY).

Colony formation

To evaluate the colony formation ability, cells were trypsinized, suspended and washed, with ice-cold PBS for three times. Subsequently, 2000 cells were plated into 6-well plates and cultured for 14 days. When the colonies were visible to the naked eye, the plate was washed with ice-cold PBS for three times. The colonies were fixed with 4% paraformaldehyde for 10 min, and stained by 0.25% crystal violet for 20 min. Each well was imaged.

Tumor formation

To evaluate the tumor formation in soft agar, cells were resuspended, washed and resuspended in 0.3% soft agar in RPMI-1640 containing 10% FBS at the final concentration of 5000 cells per well, then layered onto 0.6% solidified agar in RPMI-1640 containing 10% FBS in 6-well plates. These plates were incubated at 37°C for 14 days. Colonies containing 50 cells or more were counted using a X71 (U-RFL-T) fluorescence microscope (Olympus, Melville, NY).

RNA immunoprecipitation (RIP)

Cells were trypsinized, suspended, and washed with ice-cold PBS for three times. Then cells were lysed in RIP lysis buffer containing 100 mM KCl, 10 mM KHEPES, pH 7.2, 5 mM $MgCl_2$, 1 mM DTT, 400 μM VRC, 1 mM PMSF, 10 mM NaF, 2 mM sodium orthovanadate, 2 mM β-glycerophosphate, 0.5% IGEPAL CA-630, RNaseOUT, and protease inhibitor cocktail. The lysates were incubated on ice for 10 min and centrifuged at 14,000 rpm for 15 min to clear cell debris. The supernatants were supplemented with NT2 buffer (150 mM NaCl, 1 mM $MgCl_2$, 50 mM Tris-HCl, pH 7.4, 0.05% IGEPAL CA-630), EDTA to 15 mM, DTT to 1 mM, RNaseOUT, and then immunoprecipitated with anti-FLAG antibody prebound Dynabeads Protein G beads (Thermo Fisher Scientific, MA, USA) at 4°C overnight. The samples were washed five times with NT2 buffer supplemented with 15 mM EDTA. RNA was eluted with TRIsure (Bioline) according to the manufacturer's instructions. The isolated RNA from RIP was analyzed by quantitative PCR. The results were shown as the relative enrichment fold of anti-FLAG antibody over the Rabbit IgG antibody.

Western blot

The primary antibodies used was listed as followed: Rabbit monoclonal anti-FOXM1 antibody (1:1000, cat. No.: ab232649); Rabbit monoclonal anti-β-actin antibody (1:5000, #ab8227). Goat anti-rabbit IgG H&L antibody (HRP ladled, 1:10000, #ab7090) was used as secondary antibody. Blot bands were quantified via densitometry with Image J software (National Institutes of Health Baltimore, MD, USA). β-actin was used as an internal reference.

Statistical analysis

SPSS (software version 19.0, SPSS, Chicago, IL, USA) was employed to statistical analysis in this study. Data are presented as the mean ± standard deviation. The Student *t* test and one-way ANOVA were used to analyze 2 or multiple groups, respectively. Probabilities lower than 5% ($P<0.05$) were considered statistically significant. All experiments were repeated three or more times.

Results

LnvPVT1 was targeted and potentially regulated by miR-370 and miR-526

LncRNAs can act as a molecular sponge to impede miRNAs from binding to the mRNA targets and consequently exert as a regulator of physiological processes [21]. To predict the potential binding sites of miRNAs on PVT1, we employed RegRNA2.0 to search potential miRNA-lncRNA mutual binding and then focused on the interaction between lncRNA PVT1, miR-370-5p and miR-526-5p (**Figure 1A**), and a dual luciferase reporter assay was carried out to further confirm the specific interplay between PVT1, miR-370, and miR-526, respectively. As it is illustrated in **Figure 1B**, co-transfection of pmirGLO-PVT1 and miR-370 mimics/miR-526 mimics significantly diminished the relative luciferase activity compared with that in the pmirGLO-vector or pmirGLO-PVT1-MUT1/3, MUT2 transfected group ($P<0.05$). To further confirm the direct binding of miR-370 and miR-526 to PVT1, RNA immunoprecipitation using anti-Ago2 antibody was carried out followed by quantitative PCR (**Figure 1C**) and semi-quantitative PCR (**Figure 1D**). The results demonstrated that PVT1 was detected in immunoprecipitants in both miR-370 and miR-526 transfected

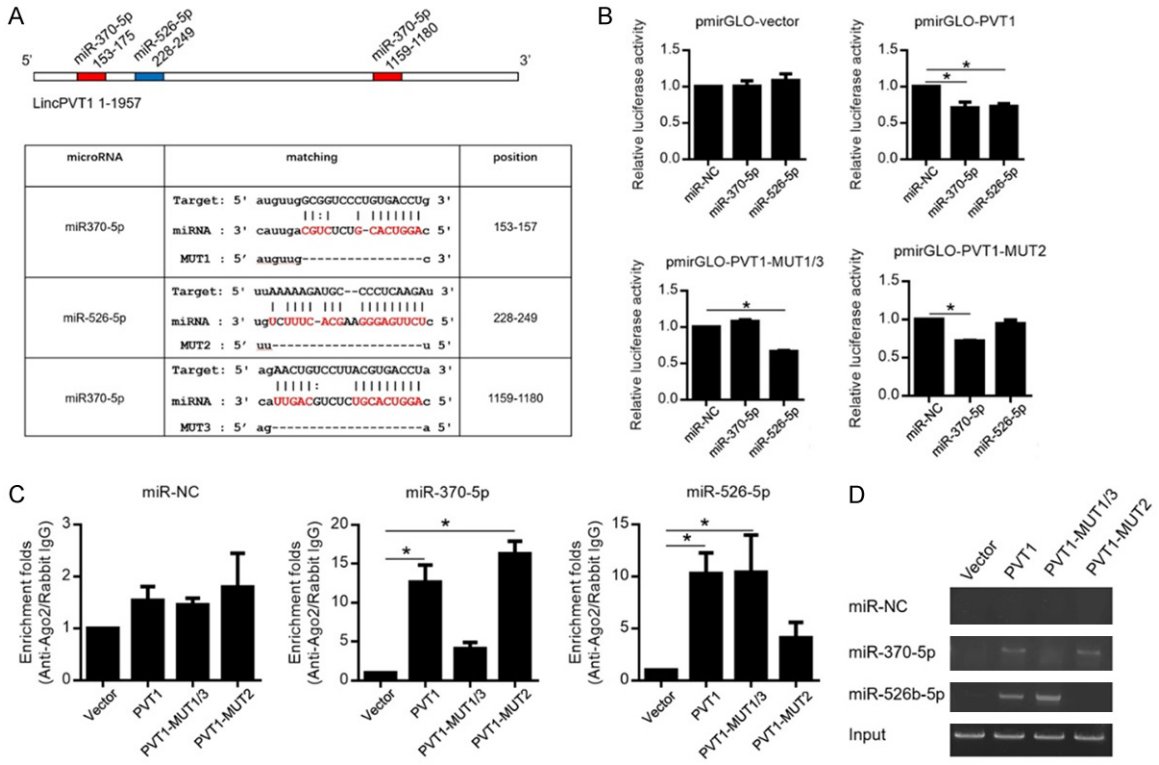

Figure 1. Prediction and confirmation of microRNAs bound to PVT1. (A) Potential binding sites of miR-370 and miR-526 on the PVT1 were predicted by using online bioinformatic tool (RegRNA2.0). The mutated binding sequences were presented for further confirming the direct binding of these two microRNAs. (B) Luciferase reporter assays were performed to demonstrate the direct binding of miR-370 or miR-526 to predicted binding sites. *P<0.05, vs. miR-NC group. RNA immunoprecipitation using anti-Ago2 antibody was performed to detect the enrichment folds of PVT1 and miR-370 followed by RT-qPCR (C) and semi-quantitative PCR (D). *P<0.05, vs. vector group.

group, indicated that binding of miR-370 and miR-526 to PVT1 potentially exert post-transcriptional regulation on PVT1.

LncPVT1, miR-370 and miR-526 are widely expressed in ovarian cancer cell lines

To detect whether LnvPVT1, miR-370 and miR-526 are widely expressed in ovarian cancer cell lines, IOSE80, SkOV3, OVCAR3, ALST and ES2 were employed for RT-qPCR analysis. As it is shown in **Figure 2A**, all these RNAs were detected efficiently in these cell lines with different expressing patterns. To detect whether the expressing level of PVT1 is correlated with the amount of miR-370 and miR-526, PVT1 was introduced into OVCAR3 and ES2, which presented the low PVT1 levels. Expectedly, overexpression of PVT1 decreased miR-370 presence in both of these two cell lines (**Figure 2B**, left and middle panel). Knockdown of PVT1 in SkOV3 significantly increased the expressing levels of both miR-370 and miR-526 (**Figure 2B**, right panel), indicated that PVT1 is negative correlated with miR-370 and miR-526.

PVT1 tightly regulates the malignant behaviors in ovarian cancer

By considering that PVT1 acts as an oncogenic molecule in multiple human cancers, including breast cancer [22], gastric cancer [23] and colorectal cancer [24], we then tried to evaluate the potential roles of PVT1 in ovarian cancer cell lines. PVT1 was introduced in ES2 cells because of its relatively low endogenous PVT1 expression and PVT1 was knockdown in SkCOV3 cells because of its relative high endogenous PVT1 expression. By detecting cell viability from day 1 to 5, overexpression of PVT1 significantly increased cell viability (**Figure 3A**) and oppositely, downregulation of PVT1 significantly decreased cell viability (**Figure 3B**), which is caused by mediating proliferating cells identified by EdU staining (**Figure 3C**). It is also presented that, by performing cell cycle analy-

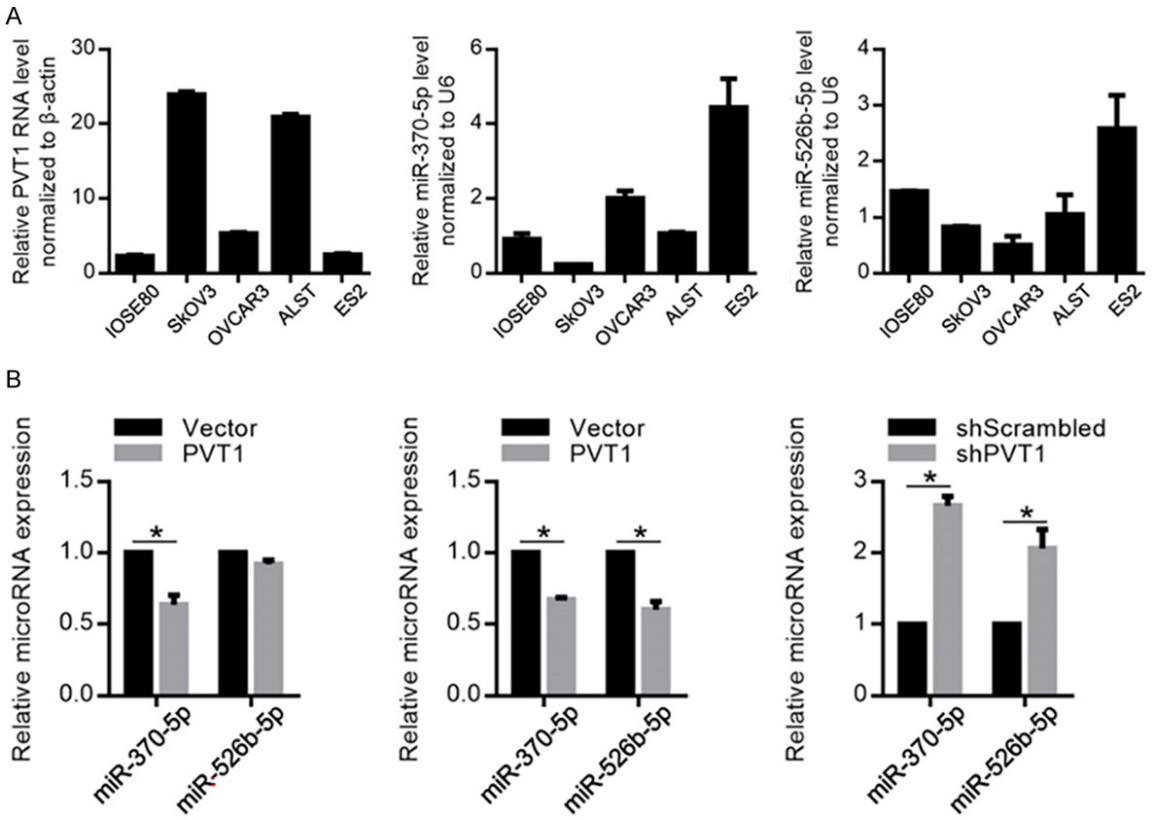

Figure 2. Relative expressing levels of PVT1, miR-370 and miR-526b in ovarian cancer cell lines. A. The relative expressing levels of PVT1, miR-370 and miR-526b were detected by RT-qPCR in IOSE80, SkOV3, OVCAR3, ALST and ES2 cell lines. B. After overexpression of PVT1 in OVCAR3 and ES2 cells, miR-370 and miR-526b were detected. After knockdown of PVT1 in SkOV3 cells, miR-370 and miR-526b were detected. *P<0.05, vs. vector or shScrambled group.

sis, the presence or absence of PVT1 is negatively correlated with the proportion of G1/G0 phase cells, indicated that PVT1 may promote cell cycle by promoting cells into S and G2 phases (**Figure 3D**).

We also detected the effects of PVT1 on other malignant behaviors, including migration, invasion, colony formation and tumor formation in ovarian cancer cells. All results demonstrated that, overexpression of PVT1 positively regulated and knockdown of PVT1 negatively regulated all these malignant behaviors (**Figure 4**). Taken together, PVT1 also exerts as a oncogenic molecule in ovarian cancer cells.

miR-370 is partially involved in PVT1-regulated proliferation

Accordingly, miR-370 is reported to be downregulated in ovarian cancer [25, 26], and overexpression of miR-370 inhibited proliferation in both SkOV3 and A2780 cells [27]. Thus, we focused on the effects of miR-370-PVT1 interaction on ovarian cancer cells. We firstly confirmed the efficacy of introduction of miR-370 mimics and the miR-370 expression after PVT1 knockdown in SkOV3 cells (**Figure 5A**). Expectedly, knockdown of PVT1 significantly decreased cell viability from day 1 to 5, which was reversed by inhibiting miR-370 via introducing miR-370 antagonist (**Figure 5B**, right panel), indicated that the promoting effect of PVT1 on proliferation is potentially via regulating miR-370. Meanwhile, introduction of miR-370 mimics significant decreased cell proliferation, further confirmed the effect of PVT1 is, at least partially, dependent on the presence of miR-370 (**Figure 5B**, left panel). This is also further confirmed by detecting cell cycle phase distribution showing that PVT1 decreased the proportion of G1/G0 via regulating miR-370 (**Figure 5C**).

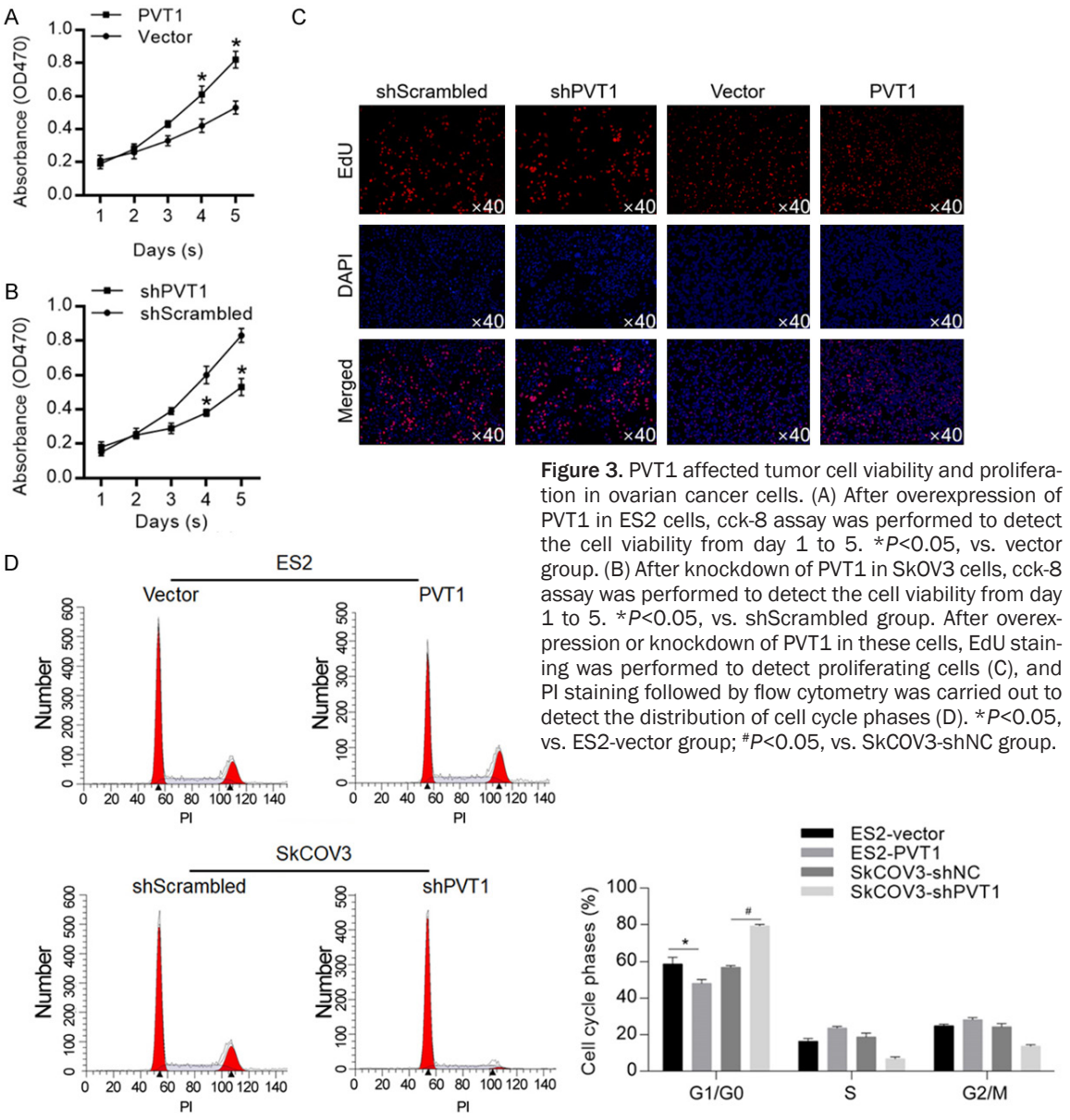

Figure 3. PVT1 affected tumor cell viability and proliferation in ovarian cancer cells. (A) After overexpression of PVT1 in ES2 cells, cck-8 assay was performed to detect the cell viability from day 1 to 5. **P*<0.05, vs. vector group. (B) After knockdown of PVT1 in SkOV3 cells, cck-8 assay was performed to detect the cell viability from day 1 to 5. **P*<0.05, vs. shScrambled group. After overexpression or knockdown of PVT1 in these cells, EdU staining was performed to detect proliferating cells (C), and PI staining followed by flow cytometry was carried out to detect the distribution of cell cycle phases (D). **P*<0.05, vs. ES2-vector group; #*P*<0.05, vs. SkCOV3-shNC group.

PVT1 tightly regulated the protein level of FOXM1

It is reported that PVT1 stabilizes the protein level of FOXM1 by directly bound [28]. This promoted us to perform chromatin immunoprecipitation after introducing Flag-tagged FOXM1, and consistent with previous report, Flag-tagged FOXM1 bound to PVT1 specifically (**Figure 6A**). By considering that miR-370 specifically target to FOXM1 mRNA and thus down-regulates FOXM1 posttranscriptional [29], we then tried to figure out whether PVT1 regulates FOXM1 in both ways. After PVT1 knockdown or introduction of miR-370 mimics, protein levels of FOXM1 were obviously decreased, which is consistent with previous finding showing that miR-370 mimics targeted to FOXM1 mRNA (**Figure 6B**). To confirm whether PVT1 stabilizes FOMX1 protein, knockdown of PVT1 and introduction of miR-137 antagonist were simultaneously achieved. As illustrated in **Figure 6C**, it is observed that knockdown of PVT1 and introduction of miR-370 mimics obviously decreased FOXM1 protein level. After inhibition of miR-370, the decrease in FOXM1 protein level resulted by knockdown of PVT1 was reversed. Taken together, PVT1 potentially maintained the protein level of FOXM1 via both stabilizing FOXM1 and abolishing miR-370.

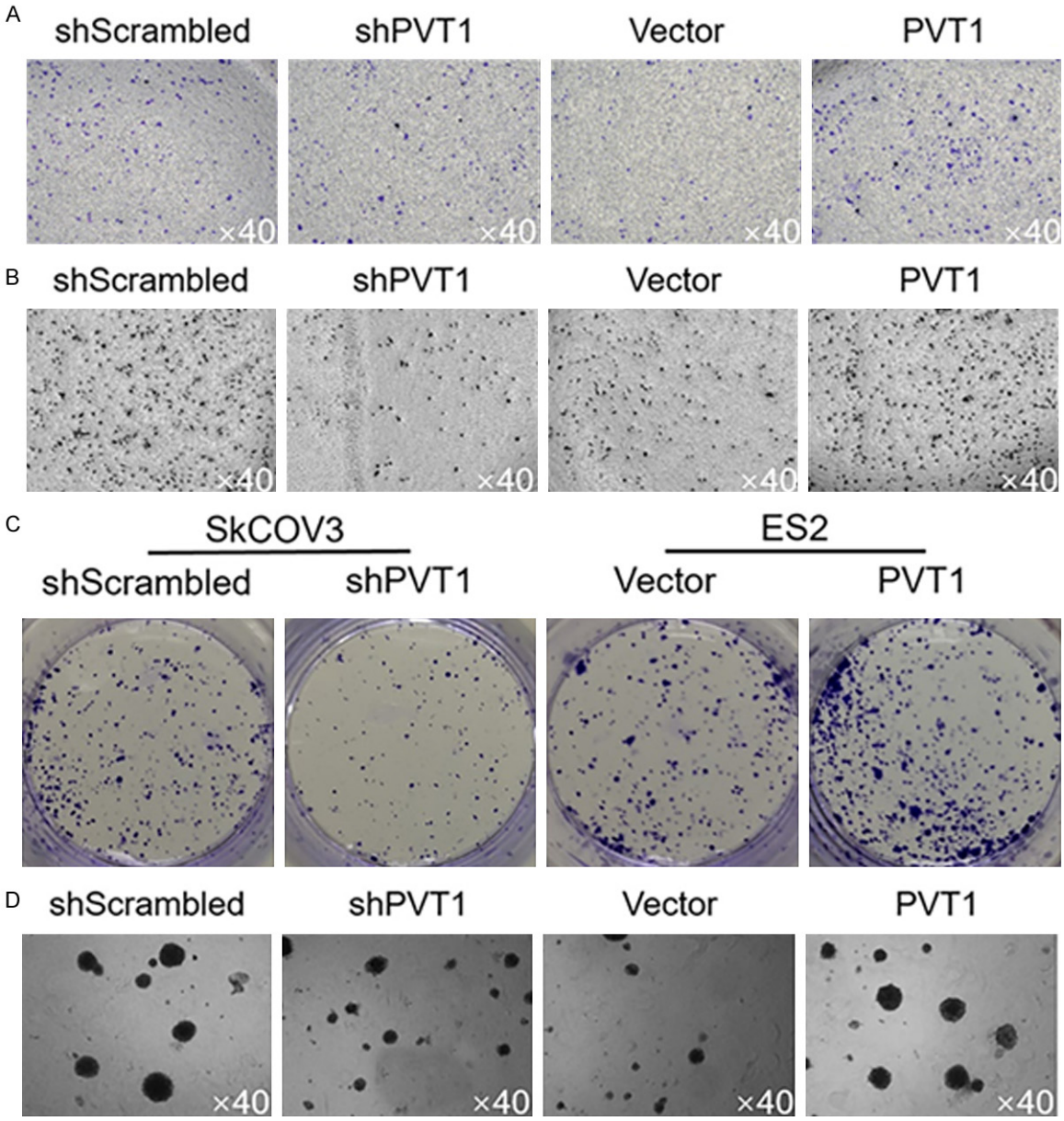

Figure 4. PVT1 affected tumor migration, invasion, colony formation and tumor formationin ovarian cancer cells. After overexpression or knockdown of PVT1 in ES2 cells or SkCOV3 cells, cells were analyzed for malignant behaviors. (A) Transwell assay without Matrigel layer was used to detect the effect of PVT1 on migration. (B) Transwell assay with Matrigel layer was used to detect the effect of PVT on invasion. Colony formation (C) and tumor formation (D) were performed.

PVT1 potentially exerts promoting effects on malignant behaviors and induced chemoresistance via regulating FOXM1

By considering that PVT1 stabilizes FOXM1 protein and protects FOXM1 mRNA from degradation by miR-370, we hypothesized that FOXM1 may play a key role in PVT1-promoted malignant behaviors. Then, we analyzed malignant behavior after FOXM1 regulation mediated by PVT1. As it is shown in **Figure 7**, knockdown of PVT1 resulted in inhibition of malignant behaviors, and was reversed by introduction of Flag-tagged FOXM1, including proliferation, migration and invasion.

SkVO3 cells are known to be resistant to platinum-based chemotherapies [30], we then tried to figure out whether PVT1, miR-370 and FOXM1 are involved in the induction of chemo-

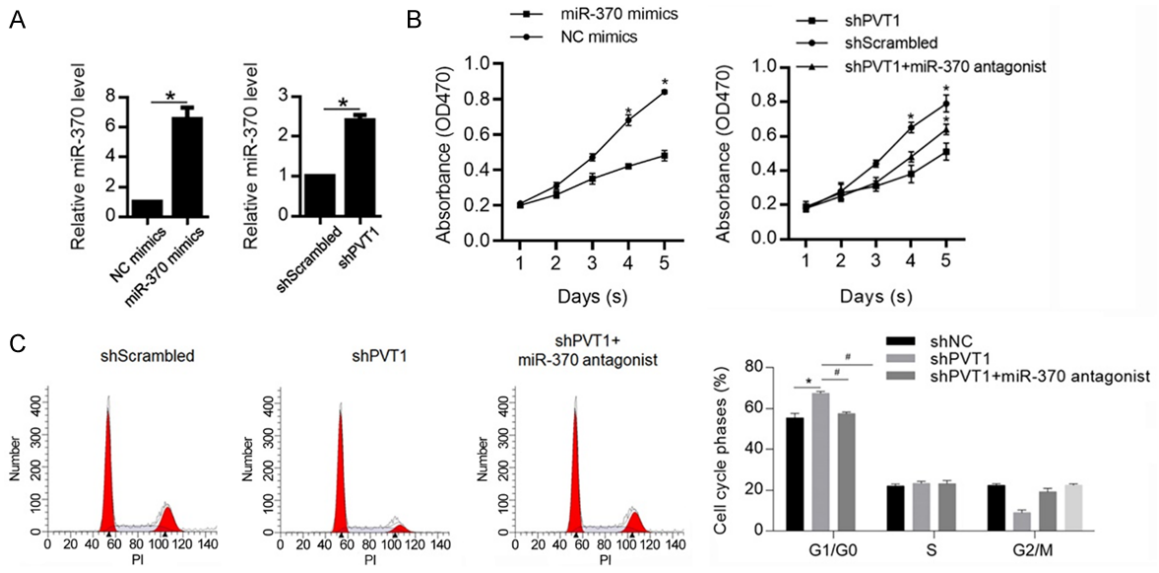

Figure 5. PVT1 positively regulated miR-370 and affected cell proliferation. (A) Introduction of miR-370 mimics significantly increased miR-370 detected by RT-qPCR. Transfection of shPVT1 obviously increased miR-370 level (right panel). **P*<0.05, vs. NC mimics group, or shScrambled group. Knockdown of PVT1 decreased cell proliferation (B) by arrest cell cycle at G1/G0 (C), which were reversed by introduction of miR-370 antagonist to block endogenous miR-370. **P*<0.05, vs. shScrambled. #*P*<0.05, vs. shPVT1 group.

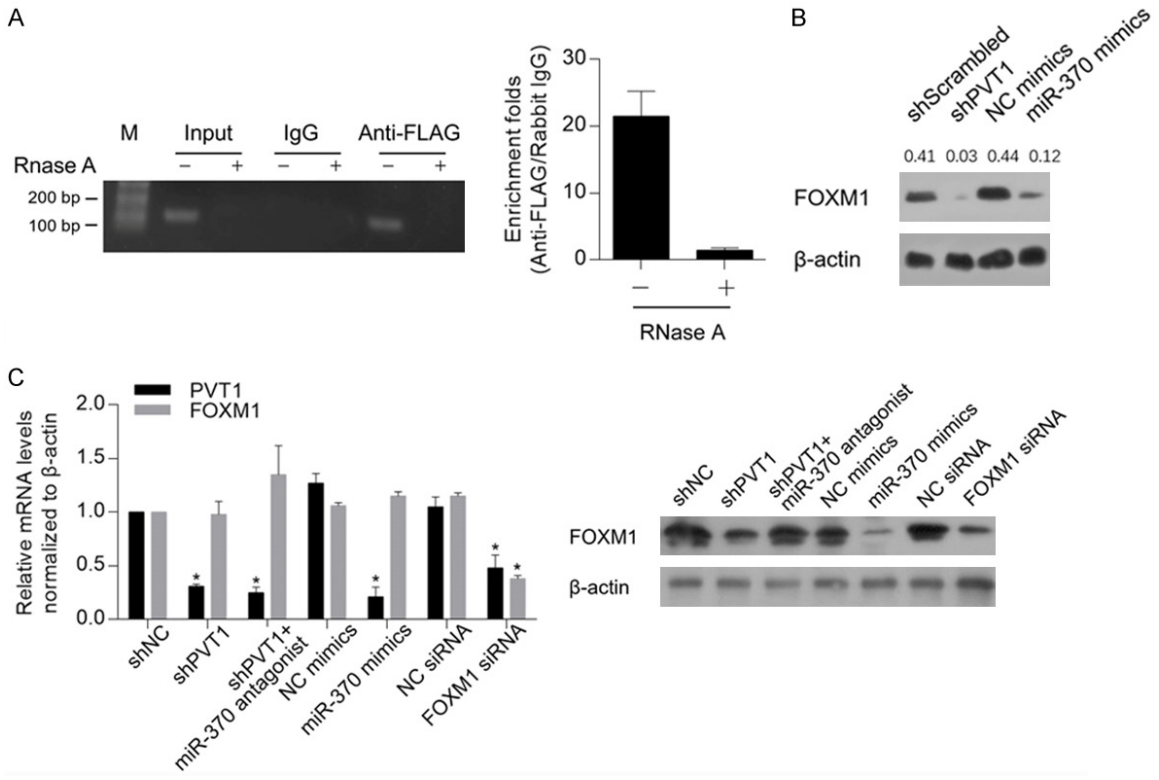

Figure 6. PVT1 bound to FOXM1 and stabilized it. A. After transfection of vector for coding Flag-tagged FOXM1 for 48 h, RNA immunoprecipitation was carried using anti-flag antibody, and PVT1 was detected by performing RT-qPCR in IP product. B. After regulation of PVT1 or miR-370, the protein level of FOXM1 was detected by semi-quantitative western blot. C. The mRNA level (left panel) and protein level (right panel) of FOXM1 was detected after regulation of PVT1 or miR-370.

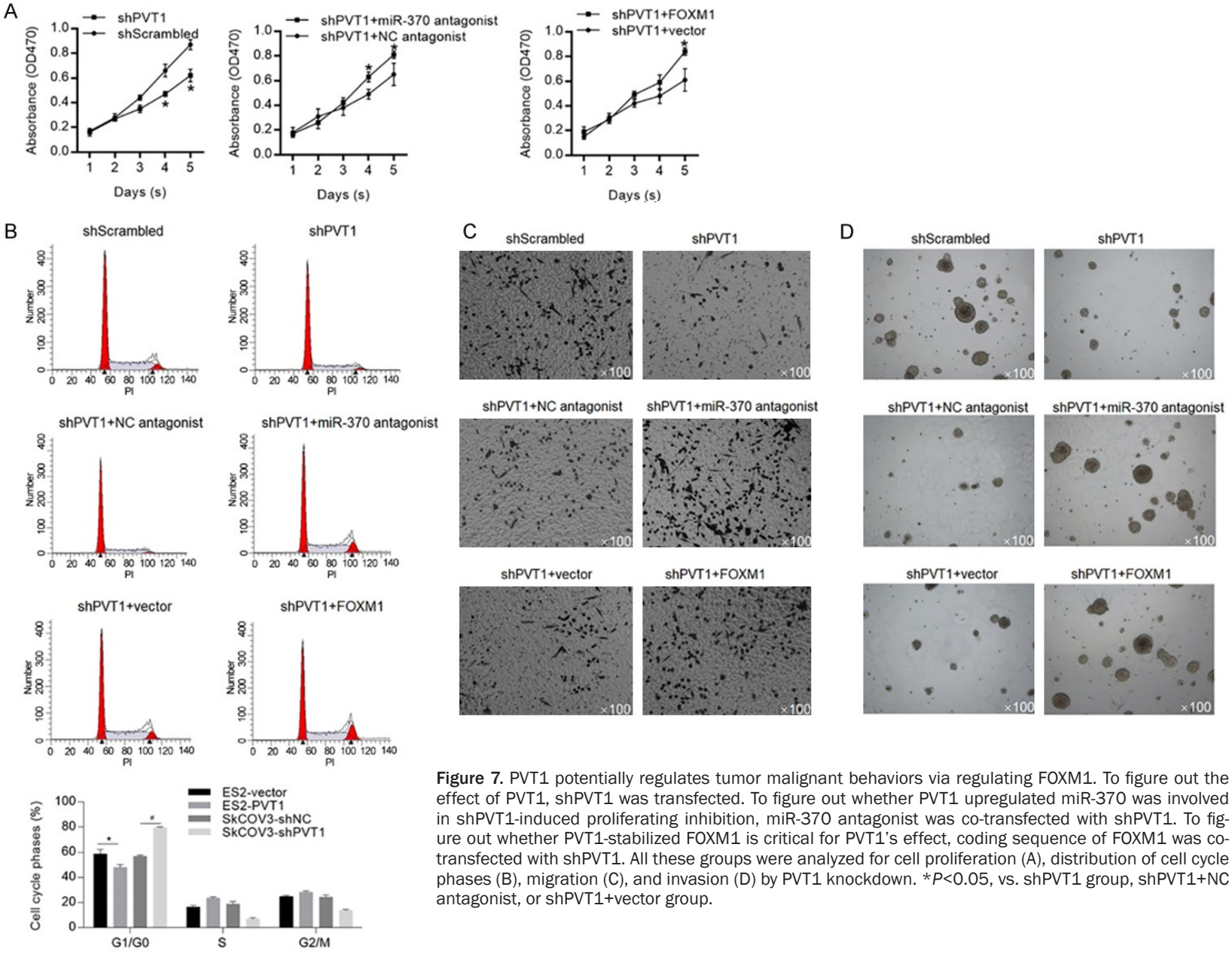

Figure 7. PVT1 potentially regulates tumor malignant behaviors via regulating FOXM1. To figure out the effect of PVT1, shPVT1 was transfected. To figure out whether PVT1 upregulated miR-370 was involved in shPVT1-induced proliferating inhibition, miR-370 antagonist was co-transfected with shPVT1. To figure out whether PVT1-stabilized FOXM1 is critical for PVT1's effect, coding sequence of FOXM1 was co-transfected with shPVT1. All these groups were analyzed for cell proliferation (A), distribution of cell cycle phases (B), migration (C), and invasion (D) by PVT1 knockdown. *P<0.05, vs. shPVT1 group, shPVT1+NC antagonist, or shPVT1+vector group.

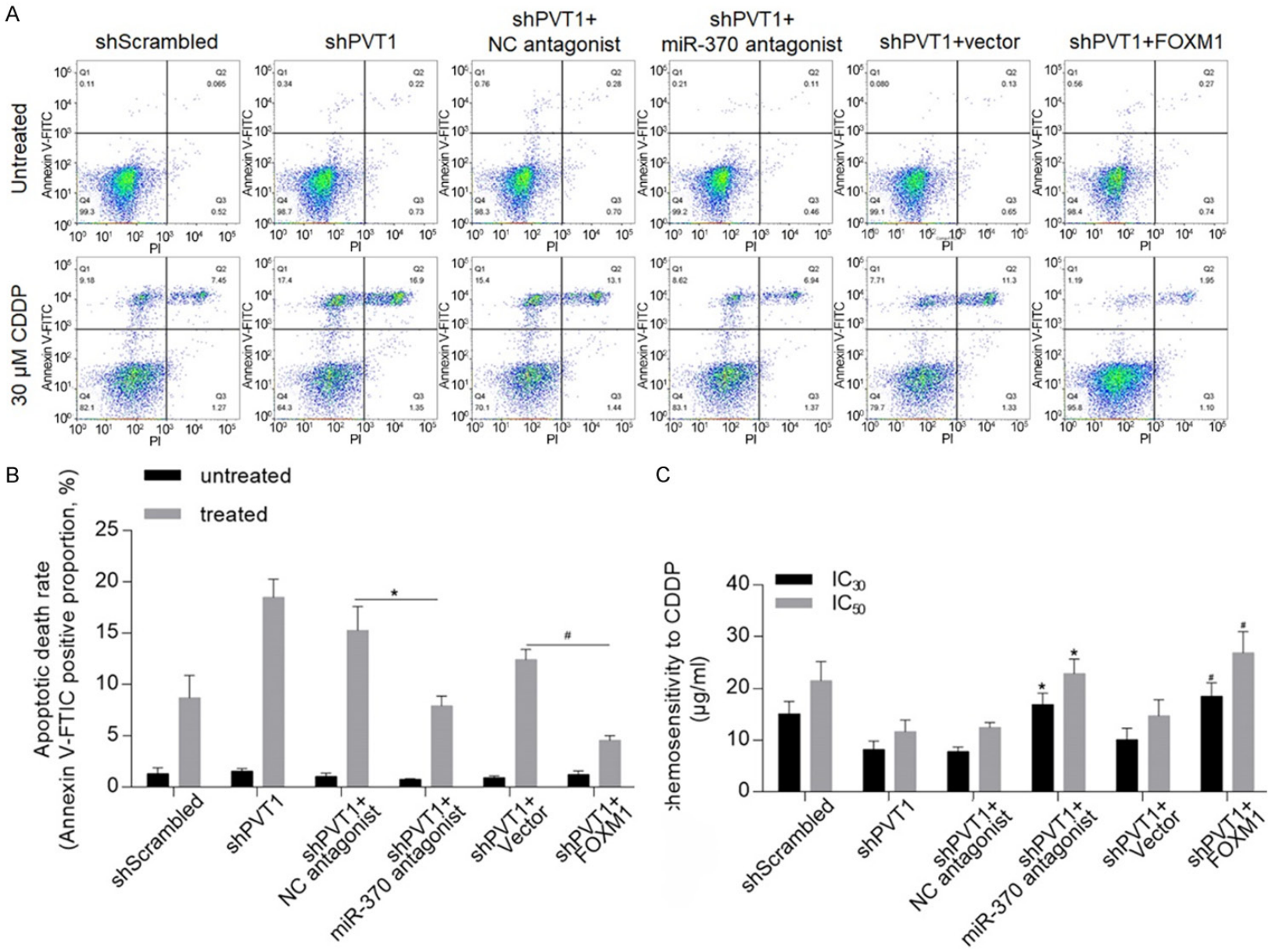
A
shScrambled
shPVT1
shPVT1+ NC antagonist
shPVT1+ miR-370 antagonist
shPVT1+vector
shPVT1+FOXM1
Untreated
30 μM CDDP
Annexin V-FITC
PI
B
untreated
treated
Apoptotic death rate (Annexin V-FTIC positive proportion, %)
shScrambled
shPVT1
shPVT1+ NC antagonist
shPVT1+ miR-370 antagonist
shPVT1+ Vector
shPVT1+ FOXM1
C
IC30
IC50
Chemosensitivity to CDDP (μg/ml)
shScrambled
shPVT1
shPVT1+ NC antagonist
shPVT1+ miR-370 antagonist
shPVT1+ Vector
shPVT1+ FOXM1

Figure 8. PVT1 potentially induced chemoresistance via regulating FOXM1 in SkOV3 against CDDP. To figure out the effect of PVT1, shPVT1 was transfected. To figure out whether PVT1 upregulated miR-370 was involved in shPVT1-induced proliferating inhibition, miR-370 antagonist was co-transfected with shPVT1. To figure out whether PVT1-stabilized FOXM1 is critical for PVT1's effect, coding sequence of FOXM1 was co-transfected with shPVT1. A and B. After 24-hour incubation with 25 μg/ml CDDP, cells were double-stained with Annexin V-FITC/PI followed by flow cytometry. **P*<0.05, vs. shPVT1+NC antagonist group; #*P*<0.05, vs. shPVT1+Vector group. C. Cell sensitivity to CDDP were confirmed by performing CCK-8 assay. **P*<0.05, vs. shPVT1+NC antagonist group; #*P*<0.05, vs. shPVT1+Vector group.

resistance to cisplatin (CDDP). As it is shown in **Figure 8A** and **8B**, knockdown of PVT1 obviously increased apoptotic rate induced by 25 μg/ml of CDDP after 24-hour treatment, which were reserved by inhibition of miR-370 or overexpression of FOXM1. Cell sensitivity to CDDP was also accessed by performing CCK-8 analysis and consistently, it is observed that knockdown of PVT1 significantly sensitized SkVO3 cells to CDDP, which was reversed by inhibition of miR-370 or overexpression of FOXM1 (**Figure 8C**). Taken together, PVT1 is critical for chemoresistance to CDDP in SkOV3 cells, which is potentially via regulating FOXM1.

Discussion

In our present study, we demonstrated that PVT1 acts as an oncogenic factor by sponging miR-370 in ovarian cancer cells. PVT1 is widely reported as a tumor promoter in several kinds of cancers. Angell and colleagues reported that in gastric cancer, PVT1 is a novel long noncoding RNA and is highly expressed in tumor tissue compared to adjacent tissue [5]. It has also been reported that in colorectal cancer, PVT1 is highly expressed in tumor tissue, and knockdown of PVT1 decreases malignant behaviors, including cell proliferation, migration and invasion [6]. In acute promyelocytic leukemia, overexpression of PVT1 is correlated with leukemic cell proliferation by suppressing MYC protein levels [7]. In addition, high PVT1 expression in cancers has also been associated with poor prognosis and mortality [31]. In ovarian cancer cells, different expression patterns of PVT1 were observed. SkOV3 cells with a high expression level of PVT1 were subjected to PVT1 knockdown, and ES2 cells with a low expression level of PVT1 were used for PVT1 overexpression. Our results showed that overexpression of PVT1 promoted malignant behaviors and that knockdown of PVT1 inhibited malignant behaviors in ovarian cancer cells and suggested that PVT1 may play an important role in ovarian cancer progression, indicating that it may be a promising therapeutic target.

In our results, PVT1 strongly and positively regulated the expression level of FOXM1, which is associated with regulation of embryogenesis [12] and organ development [13], and its upregulation was also observed in various human cancers [14, 15]. Direct binding of PVT1 to FOXM1 protein stabilized and increased FOXM1 protein levels and potentially promoted malignant behaviors, including the proliferation, migration and invasion of ovarian cancer cells. Knockdown of PVT1 decreased FOXM1 protein levels without affecting FOXM1 mRNA levels, indicating the epigenetic regulatory role of PVT1 on FOXM1 protein posttranslationally. The promoting effects of PVT1 on malignant behaviors were reversed by the introduction of miR-370 mimics and indicated that PVT1 potentially regulates malignant behaviors by stabilizing FOXM1.

Numerous studies carried by different researchers have found the critical roles of lncRNAs in physiological and pathological processes through various mechanisms [32], including in cancer progression [33]. Zhao and colleagues reported that in acute myeloid leukemia cells, the recently identified lncRNA00239 inhibited phosphorylation of the downstream signaling pathway PI3K/AKT/mTOR [34]. It has also been reported that lncRNAs may epigenetically regulate their downstream genes and thus regulate the malignant behaviors of breast cancer [35]. Mouse VL30 (mVL30) retrotransposon RNA, which is structurally similar to a retroviral genome, epigenetically regulates the DNA binding activity of PSF by binding to the RNA binding domain of PSF [36]. All of these reports indicate that lncRNAs are involved in the regulation of malignant behaviors of cancer cells via different mechanisms. Recently, lncRNAs have been found to act as competitive endogenous RNAs (ceRNAs) to inhibit miRNAs and protect target mRNAs from degradation [37]. This find-

ing prompted us to identify potential miRNA targets of PVT1 acting as a miRNA sponge. According to bioinformatic analysis, miR-370, a microRNA specifically targeting FOXM1 mRNA, was identified as a candidate, for which two binding sites were present on PVT1. This study confirmed that miR-370 bound specifically to PVT1, and its regulation of the FOXM1 protein was reserved by overexpression of PVT1. Considering that both knockdown of PVT1 and miR-370 mimics decreased FOXM1 protein levels, PVT1 potentially regulates FOXM1 protein levels not only via epigenetic binding to the FOXM1 protein but also by sponging miR-370 to promote FOXM1 mRNA translation.

Accordingly, our results demonstrated that PVT1 acts as an oncogenic factor by regulating FOXM1 protein levels in ovarian cancer cells. We also revealed that PVT1 regulates FOXM1 epigenetically and posttranscriptionally, which may provide new insight into the complexity of lncRNA regulation in cancers.

Acknowledgements

Thank Dr. Tao Hong (Sichuan University) for language editing. This study was supported by the Key research and development Subjects of Sichuan Province (grant no. 2018SZ0201).

Disclosure of conflict of interest

None.

Address correspondence to: Mingrong Xi and Jie Chen, Department of Obstetrics and Gynecology, West China Second University Hospital, Sichuan University, No. 20, Section 3, RenminNanlu Road, Chengdu 610041, Sichuan, China. Tel: +86-02885501633; Fax: +86-02885501633; E-mail: qmrjzzj@126.com (MRX); cjzb1@sina.com (JC)

References

[1] Sun M and Kraus WL. From discovery to function: the expanding roles of long non-coding Rnas in physiology and disease. Endocr Rev 2015; 36: 25-64.

[2] Zhao Z, Chen C, Liu Y and Wu C. 17beta-Estradiol treatment inhibits breast cell proliferation, migration and invasion by decreasing MALAT-1 RNA level. Biochem Biophys Res Commun 2014; 445: 388-393.

[3] Wang L, Dong P, Wang W, Huang M and Tian B. Gemcitabine treatment causes resistance and malignancy of pancreatic cancer stem-like cells via induction of lncRNA hotair. Exp Ther Med 2017; 14: 4773-4780.

[4] Yang Y, Dai W, Sun Y and Zhao Z. Long noncoding RNA linc00239 promotes malignant behaviors and chemoresistance against doxorubicin partially via activation of the PI3K/Akt/mTOR pathway in acute myeloid leukaemia cells. Oncol Rep 2019; 41: 2311-2320.

[5] Angell TE, Wirth LJ, Cabanillas ME, Shindo ML, Cibas ES, Babiarz JE, Hao Y, Kim SY, Walsh PS, Huang J, Kloos RT, Kennedy GC and Waguespack SG. Analytical and clinical validation of expressed variants and fusions from the whole transcriptome of thyroid FNA samples. Front Endocrinol (Lausanne) 2019; 10: 612.

[6] Takahashi Y, Sawada G, Kurashige J, Uchi R, Matsumura T, Ueo H, Takano Y, Eguchi H, Sudo T, Sugimachi K, Yamamoto H, Doki Y, Mori M and Mimori K. Amplification of PVT-1 is involved in poor prognosis via apoptosis inhibition in colorectal cancers. Br J Cancer 2014; 110: 164-171.

[7] Zeng C, Yu X, Lai J, Yang L, Chen S and Li Y. Overexpression of the long non-coding RNA PVT1 is correlated with leukemic cell proliferation in acute promyelocytic leukemia. J Hematol Oncol 2015; 8: 126.

[8] Wang F, Yuan JH, Wang SB, Yang F, Yuan SX, Ye C, Yang N, Zhou WP, Li WL, Li W and Sun SH. Oncofetal long noncoding RNA PVT1 promotes proliferation and stem cell-like property of hepatocellular carcinoma cells by stabilizing NOP2. Hepatology 2014; 60: 1278-1290.

[9] Tseng YY, Moriarity BS, Gong W, Akiyama R, Tiwari A, Kawakami H, Ronning P, Reuland B, Guenther K, Beadnell TC, Essig J, Otto GM, O'Sullivan MG, Largaespada DA, Schwertfeger KL, Marahrens Y, Kawakami Y and Bagchi A. PVT1 dependence in cancer with MYC copy-number increase. Nature 2014; 512: 82-86.

[10] Xu MD, Wang Y, Weng W, Wei P, Qi P, Zhang Q, Tan C, Ni SJ, Dong L, Yang Y, Lin W, Xu Q, Huang D, Huang Z, Ma Y, Zhang W, Sheng W and Du X. A positive feedback loop of lncRNA-PVT1 and FOXM1 facilitates gastric cancer growth and invasion. Clin Cancer Res 2017; 23: 2071-2080.

[11] Myatt SS and Lam EW. Targeting FOXM1. Nat Rev Cancer 2008; 8: 242.

[12] Costa RH, Kalinichenko VV, Holterman AX and Wang X. Transcription factors in liver development, differentiation, and regeneration. Hepatology 2003; 38: 1331-1347.

[13] Kim IM, Ramakrishna S, Gusarova GA, Yoder HM, Costa RH and Kalinichenko VV. The forkhead box m1 transcription factor is essential for embryonic development of pulmonary vas-

culature. J Biol Chem 2005; 280: 22278-22286.
[14] Chan DW, Yu SY, Chiu PM, Yao KM, Liu VW, Cheung AN and Ngan HY. Over-expression of FOXM1 transcription factor is associated with cervical cancer progression and pathogenesis. J Pathol 2008; 215: 245-252.
[15] Xia JT, Wang H, Liang LJ, Peng BG, Wu ZF, Chen LZ, Xue L, Li Z and Li W. Overexpression of FOXM1 is associated with poor prognosis and clinicopathologic stage of pancreatic ductal adenocarcinoma. Pancreas 2012; 41: 629-635.
[16] Cancer Genome Atlas Research Network. Integrated genomic analyses of ovarian carcinoma. Nature 2011; 474: 609-615.
[17] Lok GT, Chan DW, Liu VW, Hui WW, Leung TH, Yao KM and Ngan HY. Aberrant activation of ERK/FOXM1 signaling cascade triggers the cell migration/invasion in ovarian cancer cells. PLoS One 2011; 6: e23790.
[18] Chen Q, Zhang J, He Y and Wang Y. hsa_circ_0061140 knockdown reverses FOXM1-mediated cell growth and metastasis in ovarian cancer through miR-370 sponge activity. Mol Ther Nucleic Acids 2018; 13: 55-63.
[19] Ahmed I, Karedath T, Andrews SS, Al-Azwani IK, Mohamoud YA, Querleu D, Rafii A and Malek JA. Altered expression pattern of circular RNAs in primary and metastatic sites of epithelial ovarian carcinoma. Oncotarget 2016; 7: 36366-36381.
[20] Chen Q, Zhang J, He Y and Wang Y. hsa_circ_0061140 knockdown reverses FOXM1-mediated cell growth and metastasis in ovarian cancer through miR-370 sponge activity. Mol Ther Nucleic Acids 2018; 13: 55-63.
[21] Hou J, Wang L, Wu Q, Zheng G, Long H, Wu H, Zhou C, Guo T, Zhong T, Wang L, Chen X and Wang T. Long noncoding RNA H19 upregulates vascular endothelial growth factor A to enhance mesenchymal stem cells survival and angiogenic capacity by inhibiting miR-199a-5p. Stem Cell Res Ther 2018; 9: 109.
[22] Conte F, Fiscon G, Chiara M, Colombo T, Farina L and Paci P. Role of the long non-coding RNA PVT1 in the dysregulation of the ceRNA-ceRNA network in human breast cancer. PLoS One 2017; 12: e171661.
[23] Kong R, Zhang EB, Yin DD, You LH, Xu TP, Chen WM, Xia R, Wan L, Sun M, Wang ZX, De W and Zhang ZH. Long noncoding RNA PVT1 indicates a poor prognosis of gastric cancer and promotes cell proliferation through epigenetically regulating p15 and p16. Mol Cancer 2015; 14: 82.
[24] Ping G, Xiong W, Zhang L, Li Y, Zhang Y and Zhao Y. Silencing long noncoding RNA PVT1 inhibits tumorigenesis and cisplatin resistance of colorectal cancer. Am J Transl Res 2018; 10: 138-149.
[25] Chen XP, Chen YG, Lan JY and Shen ZJ. MicroRNA-370 suppresses proliferation and promotes endometrioid ovarian cancer chemosensitivity to cDDP by negatively regulating ENG. Cancer Lett 2014; 353: 201-210.
[26] Li J, Huang Y, Deng X, Luo M, Wang X, Hu H, Liu C and Zhong M. Long noncoding RNA H19 promotes transforming growth factor-beta-induced epithelial-mesenchymal transition by acting as a competing endogenous RNA of miR-370-3p in ovarian cancer cells. Onco Targets Ther 2018; 11: 427-440.
[27] Chen Q, Zhang J, He Y and Wang Y. hsa_circ_0061140 knockdown reverses FOXM1-mediated cell growth and metastasis in ovarian cancer through miR-370 sponge activity. Mol Ther Nucleic Acids 2018; 13: 55-63.
[28] Xu MD, Wang Y, Weng W, Wei P, Qi P, Zhang Q, Tan C, Ni SJ, Dong L, Yang Y, Lin W, Xu Q, Huang D, Huang Z, Ma Y, Zhang W, Sheng W and Du X. A positive feedback loop of lncRNA-PVT1 and FOXM1 facilitates gastric cancer growth and invasion. Clin Cancer Res 2017; 23: 2071-2080.
[29] Chen Q, Zhang J, He Y and Wang Y. hsa_circ_0061140 knockdown reverses FOXM1-mediated cell growth and metastasis in ovarian cancer through miR-370 sponge activity. Mol Ther Nucleic Acids 2018; 13: 55-63.
[30] Hou JY, Rodriguez-Gabin A, Samaraweera L, Hazan R, Goldberg GL, Horwitz SB and McDaid HM. Exploiting MEK inhibitor-mediated activation of ERalpha for therapeutic intervention in ER-positive ovarian carcinoma. PLoS One 2013; 8: e54103.
[31] Gupta RA, Shah N, Wang KC, Kim J, Horlings HM, Wong DJ, Tsai MC, Hung T, Argani P, Rinn JL, Wang Y, Brzoska P, Kong B, Li R, West RB, van de Vijver MJ, Sukumar S and Chang HY. Long non-coding RNA HOTAIR reprograms chromatin state to promote cancer metastasis. Nature 2010; 464: 1071-1076.
[32] Cech TR and Steitz JA. The noncoding RNA revolution-trashing old rules to forge new ones. Cell 2014; 157: 77-94.
[33] Liu B, Sun L, Liu Q, Gong C, Yao Y, Lv X, Lin L, Yao H, Su F, Li D, Zeng M and Song E. A cytoplasmic NF-kappaB interacting long noncoding RNA blocks IkappaB phosphorylation and suppresses breast cancer metastasis. Cancer Cell 2015; 27: 370-381.
[34] Yang Y, Dai W, Sun Y and Zhao Z. Long noncoding RNA linc00239 promotes malignant behaviors and chemoresistance against doxorubicin partially via activation of the PI3K/Akt/mTOR pathway in acute myeloid leukaemia cells. Oncol Rep 2019; 41: 2311-2320.

[35] Lv J and Zhao Z. Binding of LINE-1 RNA to PSF transcriptionally promotes GAGE6 and regulates cell proliferation and tumor formation in vitro. Exp Ther Med 2017; 14: 1685-1691.
[36] Song X, Sui A and Garen A. Binding of mouse VL30 retrotransposon RNA to PSF protein induces genes repressed by PSF: effects on steroidogenesis and oncogenesis. Proc Natl Acad Sci U S A 2004; 101: 621-626.
[37] Salmena L, Poliseno L, Tay Y, Kats L and Pandolfi PP. A ceRNA hypothesis: the Rosetta Stone of a hidden RNA language? Cell 2011; 146: 353-358.